

Experimental demonstration of optimal universal asymmetric quantum cloning of polarization states of single photons by partial symmetrization

Antonín Černoč, ¹ Jan Soubusta, ¹ Lucie Čelechovská, ² Miloslav Dušek, ² and Jaromír Fiurášek ²

¹*Joint Laboratory of Optics of Palacký University and Institute of Physics of Academy of Sciences of the Czech Republic, 17. listopadu 50A, 779 07 Olomouc, Czech Republic*

²*Department of Optics, Palacký University, 17. listopadu 12, 779 00 Olomouc, Czech Republic*

We report on experimental implementation of the optimal universal asymmetric $1 \rightarrow 2$ quantum cloning machine for qubits encoded into polarization states of single photons. Our linear optical machine performs asymmetric cloning by partially symmetrizing the input polarization state of signal photon and a blank copy idler photon prepared in a maximally mixed state. We show that the employed method of measurement of mean clone fidelities exhibits strong resilience to imperfect calibration of the relative efficiencies of single-photon detectors used in the experiment. Reliable characterization of the quantum cloner is thus possible even when precise detector calibration is difficult to achieve.

PACS numbers: 03.67.Lx, 42.50.-p

I. INTRODUCTION

Unlike classical information, quantum information cannot be freely copied. The famous quantum no-cloning theorem [1, 2] states that it is impossible to perfectly copy non-orthogonal quantum states. This puts a nontrivial bound on the ability to share quantum information among several parties which can be explored in quantum information processing applications such as quantum cryptography [3, 4]. Although perfect quantum copying is forbidden, one can nevertheless attempt to copy the quantum states in the optimal approximate manner and this has been a subject of numerous theoretical and experimental studies during the recent years [5]. Optimal quantum cloners have been identified for various sets of input states and some of them have been demonstrated experimentally [6, 7, 8, 9, 10, 11, 12, 13, 14].

Of particular interest is the optimal universal quantum cloner that should copy equally well all states from the underlying Hilbert space [6, 15, 16]. The universal quantum cloning can be accomplished by a symmetrization of a state to be cloned and a maximally mixed state of blank copies [17]. This insight has led to the experimental realization of the quantum cloning of polarization states of photons via bunching on a balanced beam splitter [8, 9, 18]. This procedure provides two clones with identical reduced density matrices and fidelities. However, one can more generally consider asymmetric quantum cloning machine that produces two clones with different fidelities F_A and F_B such that the trade-off between F_A and F_B is optimal [19, 20, 21]. Optimal asymmetric phase-covariant cloning has been demonstrated in a nuclear magnetic resonance experiment [12] and in two optical experiments involving either optical fibers and qubits encoded into path of single photons [13] or bulk optics and polarization encoding [14]. By contrast, so far only a single experimental realization of the universal asymmetric cloner has been reported. In that experiment, asymmetric cloning of polarization states of single

photons was accomplished via partial quantum teleportation [22, 23] which required detection of four-photon coincidences resulting in low coincidence rate. The performance of the cloner was thus characterized only for a rather limited set of three different input states.

Here we report on the experimental demonstration of optimal universal asymmetric cloning via the partial symmetrization of a two-photon polarization state. Our linear-optical partial symmetrizer consists in a Mach-Zehnder interferometer with additional beam splitters in its arms [24, 25]. The asymmetry of such cloner can be easily tuned by changing the transmittance of one arm of the interferometer using variable attenuator. We characterize the performance of the cloner for various degrees of asymmetry by the mean fidelities of the two clones which are experimentally determined as averages of clone fidelities for input states forming three mutually unbiased bases.

An important issue in the experiments where multiphoton coincidences are measured is the proper calibration of the relative detection efficiencies of the single photon detectors. We show that, interestingly, our method of measurement of the mean clone fidelities is inherently robust with respect to the errors in detection efficiency calibration. Even errors of the order of several ten percent can be tolerated as the resulting systematic error in determination of the mean clone fidelities is of the order of 0.5% or even smaller. This result implies that reliable estimates of certain parameters such as average fidelities can be obtained even when it is difficult to perfectly calibrate the detectors.

The rest of the paper is structured as follows. In Section II we describe the experimental setup and the measurement procedure. The experimental results are presented and discussed in Sec. III, where it is shown that our method of determination of the mean fidelities is inherently robust with respect to imperfect detector efficiency calibration. Finally, Section IV contains a brief summary and conclusions.

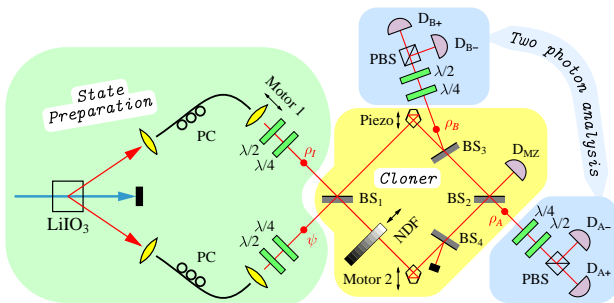


FIG. 1: (Color online) Experimental setup: PC - fiber polarization controller, BS - non-polarizing plate beam splitter, NDF - neutral density filter, PBS - polarizing cube beam splitter, $\lambda/2$ and $\lambda/4$ - wave plates, D - describes a set composed of cut-off filter, collimating lens, single-mode fiber and avalanche photodiode, DMZ - auxiliary single photon detector used for stabilization of the interferometer.

II. EXPERIMENTAL SETUP

The experimental setup for partial symmetrization of the polarization state of two photons is depicted in Fig. 1 and is described in detail in Refs. [25, 26]. In brief, correlated photon pairs are produced by the process of Type-I degenerate spontaneous parametric downconversion (SPDC) in a nonlinear crystal LiIO_3 pumped by a cw Kr-ion laser with wavelength 413 nm. The signal and idler photons are spatially filtered by coupling them into single-mode fibers. The input polarization states of the photons are prepared by means of half- and quarter-wave plates. The photons then interfere in a Mach-Zehnder interferometer supplemented by two additional beam-splitters and one neutral density filter (NDF) which serves as a polarization-insensitive attenuator. The output states of the photons are measured by means of two polarization-detection blocks consisting of a sequence of quarter- and half-waveplates, polarizing beam splitter and two single photon detectors. The device operates in the coincidence basis and the partial symmetrization is successful if a single photon is detected by each block.

As shown in Ref. [24, 25], the modified Mach-Zehnder interferometer conditionally implements a partial symmetrization operation on the polarization state of the two photons,

$$V_S = \Pi_+ + t\Pi_- \quad (1)$$

Here $\Pi_- = |\Psi^-\rangle\langle\Psi^-|$ is the projector onto the one-dimensional anti-symmetric subspace of the Hilbert space of two qubits \mathcal{H} , $|\Psi^-\rangle = \frac{1}{\sqrt{2}}(|HV\rangle - |VH\rangle)$ is the singlet Bell state and $|H\rangle$ and $|V\rangle$ denote horizontal and vertical polarization state of a single photon, respectively. Similarly, $\Pi_+ = \mathbb{1} - \Pi_-$ denotes projector onto the symmetric subspace of \mathcal{H} , $\mathbb{1}$ is the identity operator, and t denotes the amplitude transmittance of NDF. In the experiment, the interferometer is actively stabilized at

zero phase shift between the two arms which guarantees that t in Eq. (1) is real and positive. The partial symmetrization begins by a two-photon interference on the balanced beam splitter BS_1 . Photons in anti-symmetric singlet Bell state $|\Psi^-\rangle$ anti-bunch and each photon propagates through one arm of the MZ interferometer. On the other hand, if the photons are in a symmetric polarization state, then they bunch and both must propagate through the upper arm of the interferometer in order to reach the output ports. An attenuator placed in the lower interferometer arm thus selectively attenuates the anti-symmetric part of the two-photon polarization state.

In the implementation of the optimal universal asymmetric $1 \rightarrow 2$ cloning operation, the signal photon carries the state $|\psi\rangle$ that should be copied, while the idler photon represents a blank copy and is prepared in a maximally mixed state. In the experiment, this is achieved by randomly preparing the idler photon in one of the six polarization states $|H\rangle$, $|V\rangle$, $|D\rangle = \frac{1}{\sqrt{2}}(|H\rangle + |V\rangle)$, $|A\rangle = \frac{1}{\sqrt{2}}(|H\rangle - |V\rangle)$, $|R\rangle = \frac{1}{\sqrt{2}}(|H\rangle + i|V\rangle)$ and $|L\rangle = \frac{1}{\sqrt{2}}(|H\rangle - i|V\rangle)$, with equal probability $\frac{1}{6}$. The input two-photon state can thus be written as $\rho_I \otimes \psi$, where $\psi = |\psi\rangle\langle\psi|$ denotes the density matrix of a pure state $|\psi\rangle$ and $\rho_I = \frac{1}{2}(|H\rangle\langle H| + |V\rangle\langle V|)$ stands for the density matrix of a maximally mixed state. The output state of the partial symmetrizer reads

$$\rho_{\text{out}} = V_S (\rho_I \otimes \psi) V_S^\dagger = (\Pi_+ + t\Pi_-)\rho_I \otimes \psi(\Pi_+ + t\Pi_-). \quad (2)$$

After some algebra we find the following expressions for the normalized reduced density matrices of the two clones A and B, $\rho_A = \text{Tr}_B[\rho_{\text{out}}]/\text{Tr}[\rho_{\text{out}}]$, $\rho_B = \text{Tr}_A[\rho_{\text{out}}]/\text{Tr}[\rho_{\text{out}}]$,

$$\begin{aligned} \rho_A &= \frac{1}{2(3+t^2)}[(5-2t+t^2)\psi + (1+t)^2\psi_\perp], \\ \rho_B &= \frac{1}{2(3+t^2)}[(5+2t+t^2)\psi + (1-t)^2\psi_\perp]. \end{aligned} \quad (3)$$

The fidelities of the two clones, $F_A = \langle\psi|\rho_A|\psi\rangle$, $F_B = \langle\psi|\rho_B|\psi\rangle$, can be immediately determined from Eq. (3) and we obtain,

$$F_A = \frac{5-2t+t^2}{2(3+t^2)}, \quad F_B = \frac{5+2t+t^2}{2(3+t^2)}. \quad (4)$$

We can see that the transmittance t of the NDF controls the asymmetry of the cloner, i.e. the fidelities of the two clones. It can be verified that the fidelities (4) satisfy the optimal trade-off between F_A and F_B achievable by the universal $1 \rightarrow 2$ cloning machine [19, 20],

$$(1-F_A)(1-F_B) = \left(F_A + F_B - \frac{3}{2}\right)^2. \quad (5)$$

This confirms that the scheme in Fig. 1 implements the optimal asymmetric universal cloning operation.

Note that the scheme can be straightforwardly extended such as to produce, in addition to the two optimal clones, also the anti-clone [8, 9]. Instead of a single

idler photon in a maximally mixed polarization state one would have to employ a pair of photons prepared in a maximally entangled polarization singlet Bell state. One photon from this maximally entangled pair would replace the idler photon and be injected into the partial symmetrizer together with a signal photon whose polarization state should be cloned. The two partially symmetrized photons would carry the clones while the remaining photon from the maximally entangled pair would represent the anti-clone. However, such an extended setup would involve three-photon coincidence detection and would require pumping of the nonlinear crystal with femtosecond pulsed laser in order to achieve the necessary temporal synchronization and overlap of photons' wavepackets [8, 9].

In the experiment, we measure the clone fidelity for six different input states forming three mutually unbiased bases $\{|H\rangle, |V\rangle\}$, $\{|D\rangle, |A\rangle\}$, and $\{|R\rangle, |L\rangle\}$. For any basis $|\psi\rangle, |\psi_\perp\rangle$ we first set the waveplates in the detection blocks such that clicks of detectors D_{A+} and D_{B+} represent projection of photon onto polarization state $|\psi\rangle$ while clicks of D_{A-} and D_{B-} indicate projection onto state $|\psi_\perp\rangle$. We measure four two-photon coincidence rates C_{jk} of simultaneous clicks of D_{Aj} and D_{Bk} , where $j, k \in \{+, -\}$. For instance, C_{+-} always denotes number of simultaneous clicks of detectors D_{A+} and D_{B-} . For input signal state $|\psi\rangle$ the clicks of detector D_{A+} (D_{B+}) herald successful preparation of clone A (B) in state $|\psi\rangle$ and the fidelities of the two clones can thus be calculated as [11]

$$\begin{aligned} f_{A,\text{exp}}(\psi) &= \frac{C_{++} + C_{+-}}{C_{++} + C_{+-} + C_{-+} + C_{--}}, \\ f_{B,\text{exp}}(\psi) &= \frac{C_{++} + C_{-+}}{C_{++} + C_{+-} + C_{-+} + C_{--}}. \end{aligned} \quad (6)$$

We then change the input state of the signal photon to $|\psi_\perp\rangle$, while leaving the detection blocks unchanged. We again measure the four coincidence rates C_{jk} . This time a successful preparation of clone A (B) in state $|\psi_\perp\rangle$ is heralded by clicks of detector D_{A-} (D_{B-}) and the fidelities of the two clones are given by

$$\begin{aligned} f_{A,\text{exp}}(\psi_\perp) &= \frac{C_{--} + C_{-+}}{C_{++} + C_{+-} + C_{-+} + C_{--}}, \\ f_{B,\text{exp}}(\psi_\perp) &= \frac{C_{--} + C_{+-}}{C_{++} + C_{+-} + C_{-+} + C_{--}}. \end{aligned} \quad (7)$$

Note that throughout the paper we shall use lowercase f to denote fidelities of clones of single states and uppercase F to denote mean fidelities of the cloner. The mean fidelity of each clone is calculated by averaging the clone fidelities obtained for the three mutually unbiased bases,

$$\bar{F}_A = \frac{1}{6} \sum_j f_{A,\text{exp}}(j), \quad \bar{F}_B = \frac{1}{6} \sum_j f_{B,\text{exp}}(j),$$

where the summation runs over $j = |H\rangle, |V\rangle, |D\rangle, |A\rangle, |R\rangle, |L\rangle$.

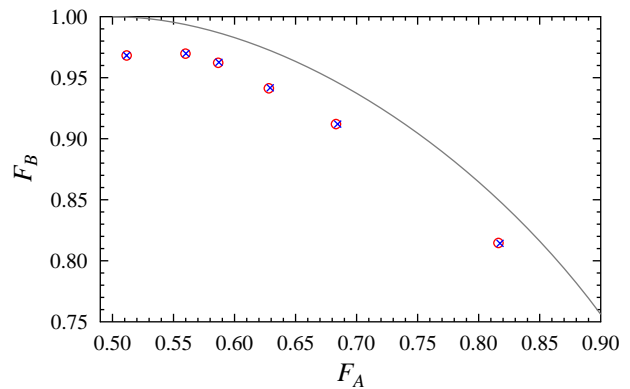


FIG. 2: (Color online) Trade-off between the fidelities of the two clones F_A and F_B . The symbols represent pairs of fidelities determined from the experimental data before calibration (red circles) and after calibration (blue crosses) of the relative detection efficiency, see main text. The solid line indicates the best possible trade-off achievable by the optimal universal asymmetric quantum cloner.

III. RESULTS AND DISCUSSION

The performance of the cloner was experimentally tested for six different degrees of asymmetry $t = \sqrt{\frac{n}{5}}$, $n = 0, 1, 2, 3, 4, 5$. The resulting mean fidelities of the two clones are plotted in Fig. 2 together with the optimal theoretical trade-off curve specified by formula (4). We can see that the cloner exhibits good performance and the experimental data follow the theoretical curve. The measured fidelities lie somewhat below the optimal theoretical bound which can be attributed mainly to the imperfect visibility of the single- and two-photon interference in our setup.

Figure 3 shows the fidelities of the first and second clones for each of the six input states. Since the cloner should be universal, one expects that for a given degree of asymmetry the fidelity should be the same for all inputs. However, a saw-like oscillatory dependence of $f_{A,\text{exp}}$ and $f_{B,\text{exp}}$ on the input state is clearly visible in Fig. 3. Namely, for each basis $|\psi\rangle, |\psi_\perp\rangle$ the fidelity of the clone A of state $|\psi\rangle$ is lower than the fidelity of the clone A of $|\psi_\perp\rangle$, while an opposite behavior is found for clone B. Taking into account our method of fidelity measurement, this can be explained by an imperfect calibration of the detection efficiencies of the employed APDs. In the experiment, we performed auxiliary measurements from which the detection efficiencies were estimated. The experimental data were then properly re-scaled. However, as Fig. 3 reveals this procedure did not completely compensate for the different efficiencies.

Since we measure coincidence rates between one detector D_{Aj} and one detector D_{Bk} , what matters are only the relative efficiencies of the two detectors in each detection block. We denote by η_A the ratio of detection efficiencies of D_{A-} and D_{A+} , and η_B is defined similarly. The

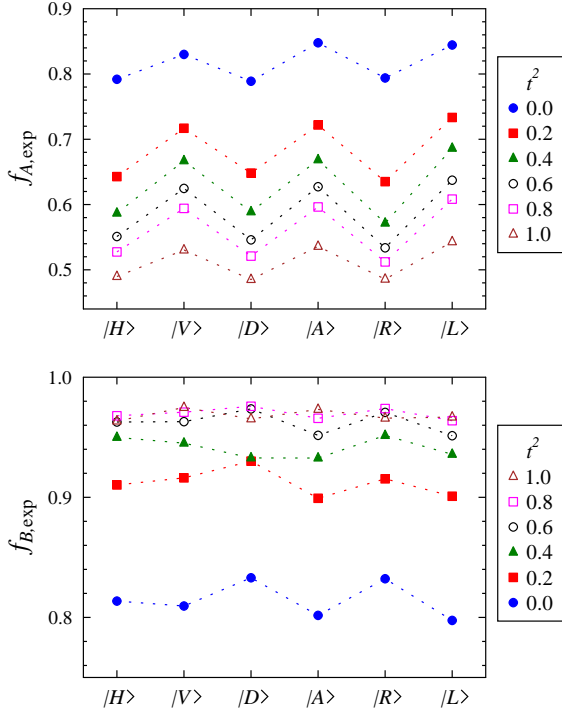


FIG. 3: (Color online) Experimentally determined fidelities of the first clone $f_{A,\text{exp}}$ (upper panel) and second clone $f_{B,\text{exp}}$ (lower panel) are plotted for each of the six input states $|\psi\rangle$ and for the six different degrees of asymmetry (see text) which are indicated by different colors and symbols.

non-unit relative detection efficiencies can be accounted for by properly rescaling the coincidence rates,

$$\begin{aligned}
 C_{++} &\rightarrow \eta_A \eta_B C_{++}, \\
 C_{+-} &\rightarrow \eta_A C_{+-}, \\
 C_{-+} &\rightarrow \eta_B C_{-+}, \\
 C_{--} &\rightarrow C_{--}.
 \end{aligned} \tag{8}$$

We can attempt to calibrate the detectors by determining η_A and η_B that minimize the spread of the fidelity for a fixed asymmetry of the cloner. We have chosen to minimize the fidelity variance defined as

$$\Delta \bar{F}_A^2 = \frac{1}{6} \sum_j f_{A,\text{exp}}^2(j) - \frac{1}{36} \left[\sum_j f_{A,\text{exp}}(j) \right]^2, \tag{9}$$

where the summation is again performed over the six input states, $j = |H\rangle, |V\rangle, |D\rangle, |A\rangle, |R\rangle, |L\rangle$. Numerical minimization of the fidelity variance yields the following values of the relative detection efficiencies,

$$\eta_A = 1.046, \quad \eta_B = 0.840. \tag{10}$$

The resulting experimental fidelities obtained from recalibrated data (8) are plotted in Fig. 4. We can see that for all degrees of asymmetry the calibration significantly reduced the spread of the fidelities, which are now practically constant and independent of the state to be cloned.

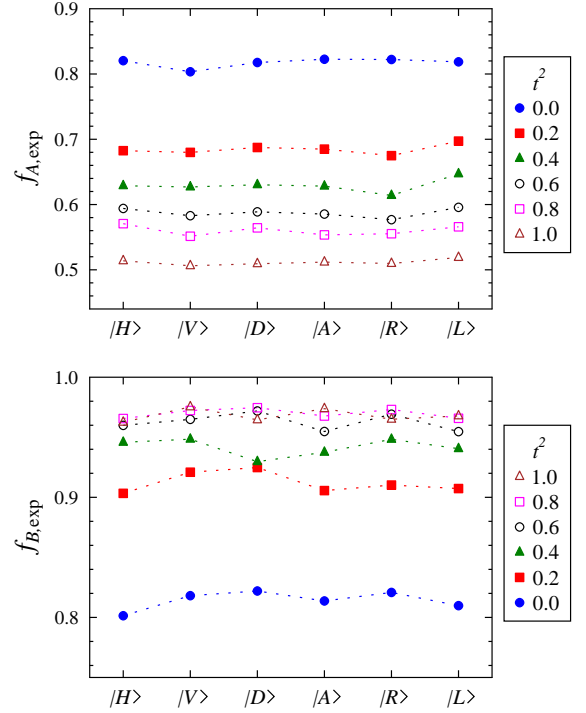


FIG. 4: (Color online) The same as Fig. 3 but the plot shows fidelities determined from the experimental data after the calibration using relative detector efficiencies given by Eq. (10).

This strongly indicates that this calibration yields reliable values of η_A and η_B .

Remarkably, the mean fidelities are almost unaffected by the calibration, as can be seen from Fig. 2. This resilience is a direct consequence of our method of measurement of the clone fidelities. The imperfect calibration results in underestimation of the fidelity $f_A(\psi)$ and overestimation of $f_A(\psi_\perp)$ (and vice versa for clone B). The mean fidelity is proportional to $f(\psi) + f(\psi_\perp)$ and this averaging significantly reduces the influence of the imperfect calibration on the final result. To show this quantitatively, we explicitly write down the dependence of the clone fidelities on η_A and η_B . Consider ideal optimal asymmetric universal quantum cloner with input state $|\psi\rangle$. The diagonal elements of the density matrix of the two clones in basis $|\psi\rangle, |\psi_\perp\rangle$ can be expressed as follows,

$$\begin{aligned}
 \rho_{\psi\psi,\psi\psi} &= P, \\
 \rho_{\psi\psi_\perp,\psi\psi_\perp} &= F_A - P, \\
 \rho_{\psi_\perp\psi,\psi_\perp\psi} &= F_B - P, \\
 \rho_{\psi_\perp\psi_\perp,\psi_\perp\psi_\perp} &= 1 + P - F_A - F_B.
 \end{aligned} \tag{11}$$

where the parameter $P = 2/(3 + t^2)$ was introduced to simplify the notation. Note, that the formula (11) does not describe only optimal universal quantum cloner but also more general class of covariant quantum machines characterized by three independent parameters F_A , F_B and P . Our analysis given below thus applies to all such machines.

The coincidence rates measured by detectors exhibiting relative detection efficiencies η_A and η_B are given by

$$\begin{aligned} C_{++} &= N\rho_{\psi\psi,\psi\psi}, \\ C_{+-} &= N\eta_B\rho_{\psi\psi_\perp,\psi\psi_\perp}, \\ C_{-+} &= N\eta_A\rho_{\psi_\perp\psi,\psi_\perp\psi}, \end{aligned}$$

$$C_{--} = N\eta_A\eta_B\rho_{\psi_\perp\psi_\perp,\psi_\perp\psi_\perp}, \quad (12)$$

where N is a constant specifying the overall coincidence rate. On inserting the expressions (11) and (12) into Eq. (6) we obtain formula for the fidelity of clone A of state $|\psi\rangle$,

$$f_A(\psi) = \frac{P + (F_A - P)\eta_B}{P + (F_A - P)\eta_B + (F_B - P)\eta_A + (1 + P - F_A - F_B)\eta_A\eta_B}. \quad (13)$$

When calculating the measured fidelity for the orthogonal input state $|\psi_\perp\rangle$ we must take into account that due to our measurement method the role of the detectors is reversed with respect to input state $|\psi\rangle$. Formally, this means that one can still use Eq. (13) but has to replace $\eta_A \rightarrow \eta_A^{-1}$ and $\eta_B \rightarrow \eta_B^{-1}$. We thus have

$$f_A(\psi_\perp) = \frac{P\eta_A\eta_B + (F_A - P)\eta_A}{P\eta_A\eta_B + (F_A - P)\eta_A + (F_B - P)\eta_B + 1 + P - F_A - F_B}. \quad (14)$$

The mean fidelity of the clone can then be calculated as average of fidelities (13) and (14),

$$\bar{F}_A = \frac{1}{2}[f_A(\psi) + f_A(\psi_\perp)]. \quad (15)$$

In order to gain insight into the dependence of \bar{F}_A on the relative efficiencies η_A and η_B we introduce new parameters ϵ_A and ϵ_B that directly quantify the relative efficiency mismatch,

$$\eta_A = 1 + \epsilon_A, \quad \eta_B = 1 + \epsilon_B, \quad (16)$$

and expand \bar{F}_A in Taylor series in ϵ_A and ϵ_B up to the second order. After some algebra we obtain

$$\begin{aligned} \bar{F}_A &\approx F_A + \frac{1}{2}F_A(1 - F_A)(1 - 2F_A)\epsilon_A^2 \\ &\quad + (2F_A - 1)(F_AF_B - P)\epsilon_A\epsilon_B \\ &\quad + \frac{1}{2}(P - F_AF_B)(1 - 2F_B)\epsilon_B^2. \end{aligned} \quad (17)$$

The terms linear in ϵ stemming from $f_A(\psi)$ and $f_A(\psi_\perp)$ exactly cancel each other so the estimation error depends only quadratically on ϵ_A and ϵ_B . Moreover, the coefficients specifying the quadratic error term in Eq. (17) are typically very small. To give a concrete example let us consider optimal symmetric universal quantum cloner. We then have

$$P = \frac{2}{3}, \quad F_A = F_B = \frac{5}{6}. \quad (18)$$

When we insert these values into Eq. (17) we obtain

$$\Delta\bar{F}_A \equiv \bar{F}_A - F_A \approx -\frac{5}{108}\epsilon_A^2 + \frac{1}{54}\epsilon_A\epsilon_B + \frac{1}{108}\epsilon_B^2. \quad (19)$$

We can bound the absolute value of the error by a maximum eigenvalue of a 2×2 matrix that describes the

quadratic form in Eq. (19),

$$|\Delta\bar{F}_A| \lesssim \frac{2 + \sqrt{10}}{108}(|\epsilon_A|^2 + |\epsilon_B|^2). \quad (20)$$

This implies that for instance a 10% error in relative calibration, $|\epsilon_A| = 0.1$, results in only a very small error in estimation of the cloning fidelity, $\Delta\bar{F}_A \approx 0.05\%$. A calculation based on the exact formulas (13) and (14) confirms this result. The analysis was presented here for clone A but similar formulas and conclusions hold also for the clone B, one only has to properly interchange labels A and B in the relevant equations.

IV. SUMMARY

In summary, we have demonstrated optimal universal asymmetric cloning of polarization states of single photons by partial symmetrization. The linear optical symmetrizer combines single- and two-photon interference in a modified Mach-Zehnder interferometer and the asymmetry of the cloner can be easily modified by inserting a variable attenuator in one arm of the interferometer. We have shown that the employed method of measurement of the mean clone fidelities has a built-in resilience against imperfect calibration of the efficiencies of the single photon detectors. This measurement procedure thus allowed a highly reliable characterization of the cloner and can be potentially useful also for characterization of other devices such as linear optical quantum gates.

Acknowledgments

This research was supported by the projects LC06007, 1M06002 and MSM6198959213 of the Ministry of

-
- [1] W.K. Wootters and W.H. Zurek, *Nature (London)* **299**, 802 (1982).
- [2] D. Dieks, *Phys. Lett. A* **92**, 271 (1982).
- [3] N. Gisin, G. Ribordy, W. Tittel, and H. Zbinden, *Rev. Mod. Phys.* **74**, 145 (2002).
- [4] V. Scarani, H. Bechmann-Pasquinucci, N.J. Cerf, M. Dušek, N. Lütkenhaus, and M. Peev, *Rev. Mod. Phys.* **81**, 1301 (2009).
- [5] V. Scarani, S. Iblisdir, N. Gisin, and A. Acin, *Rev. Mod. Phys.* **77**, 1225 (2005).
- [6] A. Lamas-Linares, C. Simon, J.C. Howell, and D. Bouwmeester, *Science* **296**, 712 (2002).
- [7] H.K. Cummins, C. Jones, A. Furze, N.F. Soffe, M. Mosca, J.M. Peach, and J.A. Jones, *Phys. Rev. Lett.* **88**, 187901 (2002).
- [8] M. Ricci, F. Sciarrino, C. Sias, and F. De Martini, *Phys. Rev. Lett.* **92**, 047901 (2004).
- [9] W.T.M. Irvine, A. Lamas-Linares, M.J.A. de Dood, and D. Bouwmeester, *Phys. Rev. Lett.* **92**, 047902 (2004).
- [10] J. Du, T. Durt, P. Zou, H. Li, L. C. Kwek, C. H. Lai, C. H. Oh, and A. Ekert, *Phys. Rev. Lett.* **94**, 040505 (2005).
- [11] A. Černocho, L. Bartůšková, J. Soubusta, M. Ježek, J. Fiurášek, and M. Dušek, *Phys. Rev. A* **74**, 042327 (2006).
- [12] H. Chen, X. Zhou, D. Suter, and J. Du, *Phys. Rev. A* **75**, 012317 (2007).
- [13] L. Bartůšková, M. Dušek, A. Černocho, J. Soubusta, and J. Fiurášek, *Phys. Rev. Lett.* **99**, 120505 (2007).
- [14] J. Soubusta, L. Bartůšková, A. Černocho, M. Dušek, and J. Fiurášek, *Phys. Rev. A* **78**, 052323 (2008).
- [15] V. Bužek and M. Hillery, *Phys. Rev. A* **54**, 1844 (1996).
- [16] N. Gisin and S. Massar, *Phys. Rev. Lett.* **79**, 2153 (1997).
- [17] R.F. Werner, *Phys. Rev. A* **58**, 1827 (1998).
- [18] I.A. Khan and J.C. Howell, *Phys. Rev. A* **70**, 010303 (2004).
- [19] N.J. Cerf, *Phys. Rev. Lett.* **84**, 4497 (2000).
- [20] C.-S. Niu and R. B. Griffiths, *Phys. Rev. A* **58**, 4377 (1998).
- [21] S. Iblisdir, A. Acin, N. J. Cerf, R. Filip, J. Fiurášek, and N. Gisin, *Phys. Rev. A* **72**, 042328 (2005).
- [22] R. Filip, *Phys. Rev. A* **69**, 052301 (2004).
- [23] Z. Zhao, A.-N. Zhang, X.-Q. Zhou, Y.-A. Chen, C.-Y. Lu, A. Karlsson, and J.-W. Pan, *Phys. Rev. Lett.* **95**, 030502 (2005).
- [24] J. Fiurášek and N.J. Cerf, *Phys. Rev. A* **77**, 052308 (2008).
- [25] A. Černocho, J. Soubusta, L. Bartůšková, M. Dušek, and J. Fiurášek, *New J. Phys.* **11**, 023005 (2009).
- [26] A. Černocho, J. Soubusta, L. Bartůšková, M. Dušek, and J. Fiurášek, *Phys. Rev. Lett.* **100**, 180501 (2008).